Underwater Images Enhancement Using Multi-Wavelet Transform and Median Filter

Mingwei Sheng*, Yongjie Pang, Lei Wan, Hai Huang
National Key Laboratory of Science and Technology of Underwater Vehicle/Harbin Engineering University,
145 Nantong Street, Harbin, 150001, China
*Corresponding author, e-mail: smwsky@163.com

Abstract

Autonomous underwater vehicles (AUV) are usually equipped with vision sensors. However, the underwater images captured by AUV often suffer from effects such as diffusion, scatter and caustics. So image enhancement methods are necessary to increase visual quality. A Median filter de-noising approach based on multi-wavelet transform was proposed to remove the impulse noise viewed as random noise from the blurred underwater image. Biorthogonal muti-wavelet has two scaling functions that may generate different multiresolution analysis, so it was chosen as the basic wavelet for underwater image two-layer decomposition and reconstruction. On this basis, the blurred underwater image was decomposed and reconstructed adopting Biorthogonal and the Median filter was applied for removing the impulse noise form the decomposition images of each layer. Four indexes were involved to evaluate the performance of de-noising. The results show that the proposed approach provides superior results compared to other de-noising method.

Keywords: image enhancement, underwater image de-noising, biorthogonal basic wavelet transform, median filter

1. Introduction

Computer vision has recently increasingly been considered as a sensing modality for underwater vehicles used in tasks such as accurate measures [1], seabed reconstruction, pipeline inspection [2], and object tracking [3]. The special transmission properties of the light in the underwater medium are always viewed as a major obstacle to processing underwater images. In the aquatic environment light suffers two different properties: absorption and scattering, which generate some problems in underwater images, such as blurring, low-contrast and noise [4]. Image De-noising is necessary for some specific applications, and the de-noised image should be more suitable for computer subsequent treatment and other perception.

The maindrawback of employing optical cameras in underwater applications is limited visibility that can be restricted to about twenty meters in clear water and less than a few meters in turbid and coastal waters [5]. The quality of images acquired under the sea can be poor because of specific propagation properties of light in water, so image enhancement is necessary to enable effective interpretation means for operators. For underwater images enhancement, the goal is to accentuate certain image features for subsequent analysis or for image display. Examples include contrast and edge enhancement, pseudo coloring, noise filtering, sharpening and magnifying. Image enhancement is useful in feature extraction, image analysis and visual information display. The enhancement process itself does not increase the inherent information display in the data. It simply emphasizes certain specified image characteristics. Enhancement algorithms are generally interactive and application dependent [6].

As a result of generated noise in the underwater image, the image quality and contrast are both decreased. The key issue for de-noising is how to choose a degradation model of blurred image. There are many different techniques applied for improving the image quality, such as Fourier domain techniques, regularization methods, recursive, iterative filters, weighted average method and etc. However, the quality of images acquired using these techniques can be poor because the approximate parameters of the blurred image are unknown [7, 8]. In some applications, such as bone age detection in medical inspection and selecting athletes, medical

diagnosis, satellite imaging, estimating of blurred image extent and etc, image de-noising also plays an important role [9-12].

Wavelet transform is considered convenient in selecting base with multi-resolution, and have low-entropy, decorrelation characters, which is useful for the protection and extraction of the edge features. Many image de-noising algorithms based on the wavelet transform have been raised during last decades. Mallat fast algorithm with using the directivity and non redundancy of wavelet decomposition, can fuse images pertinently in the feature fields of each layer through multi-resolution analysis. These kinds of algorithms effectively extract the structure and the detail information of source images, and the visual effectiveness using the image de-noising algorithm based on the wavelet transform is better than former methods. In this paper, based on the discrete multi-wavelet transform, a Madian filter approach for the restoration of defocus the impulse noise image was proposed.

The organization of the paper is as follows: In Section 2 the impulse noise of underater images is explained. The theory of wavelet transform and multi-wavelet algorithm are briefly surveyed, and two filter algorithms are described in Section 3. For giving an impersonal remark on the performance of the image de-nosing, four evelution indexes are involved in Section 4. Section 5 presents the test data sets and the results of the blurred underwater image de-noising. Matlab is used to assess the efficiency of the algorithm for the multi-wavelet transform and image fliter objectively and subjectively. Finally, summary and conclusion are given.

2. Impulse noise

Image noise is considered as an impediment to human visual perception. Varieties of factors hinder the system image sensor to acquire original image information, or can also be considered as the deviation between the ideal signal and the true signal. A noise is generally a random and unpredictable signal, so a statistical point of view can be mathematically used to define the noise. Noise of the image affects the entire process of the image processing that include the input, collection, processing and output of the results. Especially when the input is accompanied by a large noise, the noise inevitably affects the entire process and output results.

Impulse noise is always considered as the random noise reflected in the underwater image. The probalilty density functions (PDF) of impulse noise is given by:

$$p(z) = \begin{cases} p_a & for \quad z = a \\ P_b & for \quad z = b \\ 0 & otherwise \end{cases} \tag{1}$$

Where z represents gray level. If $b > a$, gray-level b will appear as a light dot in the image. Conversely noise will appear like a dark dot. If either P_a or P_b is zero, the impulse noise is called uni-polar. If neither probability is zero and especially if they are approximately equal impulse noise values will resemble salt-and-pepper granules randomly distributed over the image. For this reason bipolar impulse noise is also called salt-and-pepper noise. Shot and spike noise terms are also used to refer this type of noise.

Noise impulses can be negative or positive. Scaling usually is part of the image digitizing process. Because impulse corruption usually is large compared with the strength of the image signal, impulse noise generally is digitized as extreme (pure white or black) values in an image. Thus the assumption usually is that a and b are "saturated" values in the sense that they are equal to the minimum and maximum allowed values in the digitized image. As a result, negative impulses appear as black (pepper) points in an image. For the same reason, positive impulses appear white (salt) noise. For an 8-bit image this means that $a = 0$ (black) and $b = 255$ (white).

The original image is shown in Figure 1, and its size is 400×300. Figure 2 is the blurred image with impulse noise (salt and pepper noise) whose variance is 0.02.

Figure 1. Original Image   Figure 2. Blurred Image Consisting Impulse Noise

3. Wavelet Transform and Filter Algorithm
3.1. Wavelet Transform
Wavelet transform technology is widely used in the field of image processing and has already become an efficient tool for image processing. Wavelet transform includes mainly two kinds: continuous wavelet transform and discrete wavelet transform. Direct calculation of the two-dimension continuous wavelet transform (DTCWT) of an image requires great amount of time and computer resources. The fast-Fourier-transform method (FFT) and inverse FFT are always necessary to compute convolution for making such calculations practically possible and reducing its time considerably. While discrete wavelet transform can be divided into orthogonal basis and many generalization forms, which is widely used based on multi-resolution, and can be written into digital filter. So discrete wavelet transform is an efficient algorithm for coding and data compression.

3.2. Definition of Discrete Wavelet Transform
Supposing that function $\Psi(x) \in L^2(R)$ (in which L^2(R) represents mean square integratable one-dimension function's Hilbert space) satisfies permission condition:

$$\int_{-\infty}^{+\infty} \Psi(x)dx = 0 \tag{2}$$

The function $\Psi(x)$ is named as wavelet function. If we compress and expand the function $\Psi(x)$ by making use of s which named scale factor, the function can be obtained as following:

$$\Psi_s(x) = \frac{1}{s}\Psi(\frac{x}{s}) \tag{3}$$

Then the definition of wavelet transform on the scale s and position x is as following:

$$W_s f(x) = f(x) * \Psi_s(x) = \int_{-\infty}^{+\infty} f(u)\Psi_s(x-u)du \tag{4}$$

Where '$*$' means convolution, s takes consecutive valued among real domain. For convenient, we can take values discretely in cardinal number 2 fashions, $s=2^j$ ($j \in Z$, Z represents the integer set), then the definition of cardinal number 2 wavelet is:

$$\Psi_2^j(x) = \frac{1}{2^j}\Psi(\frac{x}{2^j}) \tag{5}$$

The wavelet transform of function $f(x)$ on the scale s and position x is:

$$W_2^j f(x) = f(x) * \Psi_2^j(x) \tag{6}$$

Function sequence $Wf = \{W_2^j f(x)\}$ $j \in Z$ is called binary wavelet transform of $f(x)$.

3.3. Algorithm of Discrete Wavelet Transform and Multi-wavelet

One kind of fast algorithm for discrete binary wavelet transform was raised by Mallat [13]. Different to the original data in a stack step by step, Mallat used a low-pass filter *H* and a high-pass filter *G* instead. The Mallat algorithm is defined as following:

$$W_2^{j+1}h = S_2^j h * G_j \tag{7}$$

$$S_2^{j+1}h = S_2^j h * H_j \tag{8}$$

Where *G* and *H* are filtering coefficients corresponding to the wavelet function's high-pass and low-pass filters separately. G_j and H_j represent discrete filters which come from inserting 2^j-1 zero in the neighboring coefficients between *G* and *H*.

As a kind of coefficient decomposition and synthesis algorithm based on the analysis of multi-resolution, the algorithm adopts tower-style decomposition and synthesis structure. The algorithm essence is a fast algorithm which can be used to break down and make up the original data again by only using the coefficients but not needing to know the scale function and the particular structure of wavelet function.

For example, considering an original image as an initial signal consisting of delicate details, it can be divided into two parts: low-frequency (fuzzy) part and high frequency (edge) part, then the course of wavelet-decomposition and synthesis can be considered as the course of half-filter and double-filter. As is shown in Figure 3, *H*, *G*, *H*[*], *G*[*] are digital filters, 2↓ is half-filter, 2↑ is double-filter.
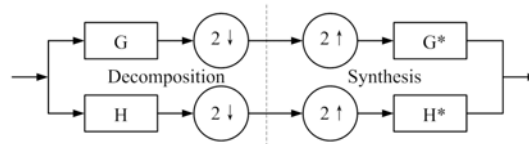

Figure 3. Wavelet Decomposition and Synthesis

Multi-wavelet is a natural promotion of a single wavelet, which has characters such as orthogonality, symmetry, short support, and high vanishing moments. And in the practical application of image processing, it is of importance for an analysis tool to possess both orthogonality (to maintain energy) and symmetry (linear phase) properties. Through the active explorations in image processing applications, certain achievements have been made, such as still image compression, coding, de-noising and etc.

It is convenient to name the biorthogonal wavelets as bior$N_a.N_b$, where N_a is the number of the order of the wavelet or the scaling functions used for reconstruction, while N_b is the order of the functions used for decomposition. The support width of the reconstruction and decomposition functions is $2N_a$+1 and $2N_b$+1, respectively. The length of the associated filters is max $(2N_a, 2N_b) + 2$.

3.4. Median Filter Algorithm

The best known order-statistics filter is the Median filter, which replaces the value of a pixel by the Median of the gray levels in the neighborhood of that pixel $f'(x, y)$ is defined as follow:

$$f'(x, y) = \underset{(s,t) \in S_{xy}}{median} \{g(s,t)\} \tag{9}$$

The original value of the pixel is included in the computation of the Median. For some random noise, the Median filter can provide excellent noise reduction capabilities, with considerably less blurring than linear smoothing filters of similar size [14, 15]. So Median filter was invovled and adopted for removing the impulse form the blurred underwater image.

3.5. Wiener Filter Algorithm

In Wiener filter algorithm, information about the noise variance is necessary to good quality restoration. However, mismatching filter variance parameter to actual noise variance causes significant degratation of filter's performance. The main drawback of Wiener filter is the necessity of a priori knowledge of type and magnitude of noise, which is often unavailable or hardly accessible in practice.

4. The Objective Evaluation Criteria of Underwater Image De-noising

According to the visual effect, the qualitative comparison is necessary to analyze the performance of de-noising. Because the human eyes are dramatic sensitive to the changing local part in an image, it's an important standard for the qualitative judgment that whether the edge and corner is obvious or not. Four indexes (Entropy, the Peak Signal to Noise Ratio, the Normalized Mean Squared Error and the Root Mean Square) were adopted for evaluating the performance of underwater image de-noising algorithms. The indexed are defined as follows:

a) Entropy (H): the value of Entropy represents the size of evaluate amount of information, it was defined as:

$$H = -\sum_{i=0}^{L-1} P_i \log(P_i) \tag{10}$$

In the formula: L is the level of the gray value. P_i is the probability density of pixel i.

b) PSNR: the Peak Signal to Noise Ratio (PSNR) indicates the effectiveness of this algorithm. The PSNR (dB) can be written as follow:

$$PSNR = 10 \log_{10} \frac{255^2}{\dfrac{1}{MN} \sum_{i=0}^{N-1} \sum_{j=0}^{M-1} [f(x,y) - g(x,y)]^2} \tag{11}$$

Where M is the width of image and N is the height of image, $f(x, y)$ is the gray scale value of original image, and $g(x, y)$ is the gray scale value of the de-noised image.

c) NMSE: As a measure of the quality of the de-noised image, the Normalized Mean Squared Error (NMSE) is also used in the experiment. NMSE in decibels is given by:

$$NMSE = \frac{\sum_{i,j} [f(i,j) - g(i,j)]^2}{\sum_{i,j} f^2(i,j)} \tag{12}$$

Where $f(x, y)$ is the gray scale value of original image, and $g(x, y)$ is the gray scale value of the de-noised image.

d) RMS: the Root Mean Square (RMS) is also involved to indicate the effectiveness of this algorithm. RMS was written as follow:

$$RMS = \sqrt{\frac{\sum_{i,j} [f(i,j) - g(i,j)]^2}{MN}} \tag{13}$$

Where M is the width of image and N is the height of image, $f(x, y)$ is the gray scale value of original image, and $g(x, y)$ is the gray scale value of the de-noised image.

5. Results and Analysis
5.1. Second Generation Biorthogonal Decomposition

In this experiment, Biorthogonal multi-wavelet (bior3.7) was chosen as basic wavelet for decomposition and reconstruction of the blurred image with the impulse noise. The number of image decomposition layer is two. Experimental decomposited images of each layer are shown as Figure 4.
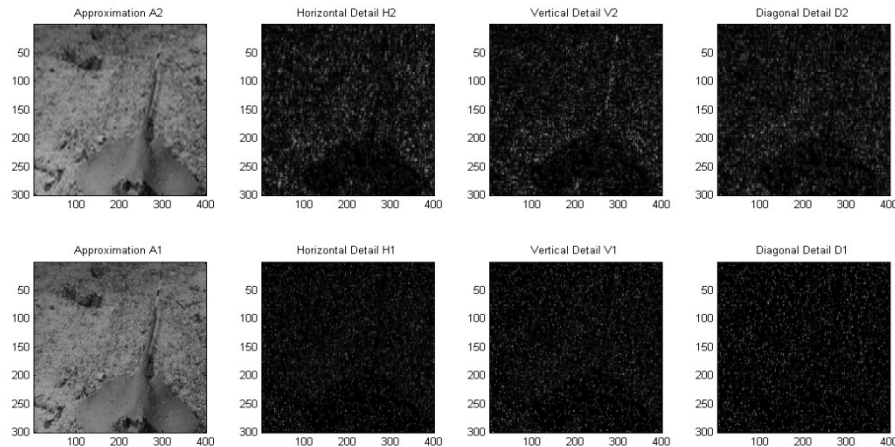

Figure 4. Biorthogonal Multi-wavelet Two-level Decomposition Images

Figure 4 demonstrates that the low-frequency spatial information focuses in A1 and A2, and the high-frequency spatial information scatters in other images. The latter also possesses orientation property and distributes according to horizontal (H1, H2), vertical (V1, V2) and planer diagonal (D1, D2) directions.

5.2. Underwater Image Filter Results Analysis

For testing the effectiveness of the de-noising algorithms, there are two comparison experiments carried out for removing the impulse noise from the blurred images (Figure 2). The Median filter and Wiener filter were respectively chosen to filter the blurred image. Figure 5 shows the experimental results of different filters. Experimental results demonstrate that the Wiener filter algorithm had the blurred edge with slat and pepper noise, but the Median filter algorithm achieved desired de-noising effectiveness and preserved the better edge information of the original image.
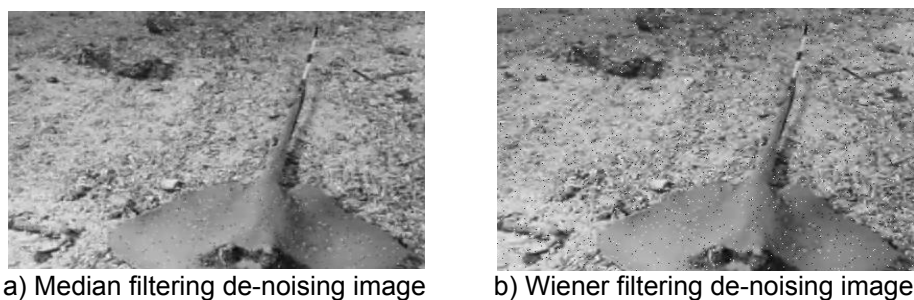

a) Median filtering de-noising image   b) Wiener filtering de-noising image

Figure 5. Comparison Experimental Analyses of Different Filtered Images

5.3. Comparison of Different De-noising Algorithms

The evaluation criteria parameters of the two kinds of de-noising algorithms (Median filter and Wiener filter) are all illustrated in Table 1.

Table 1. Evaluation Criteria Parameters

Restoration Methods	Noise Image	Median filtered image	Wiener filtered image
H	7.331	7.1523	7.2645
PSNR (dB)	70.4724	76.2141	71.4733
NMSE	0.0173	0.0046	0.0681
RMS	0.0764	0.0394	0.0681

As was shown in Table 1, from the experiment results, although Entropy (*H*) coefficients of Wiener filter algorithm is little larger than that of Median filter method, the Median filter can acquire lager PSNR and smaller NMSE and RMS. The performance of Median filter is better both in qualitative and quantitative analysis.

6. Conclusion

An algorithm for the restoration of defocus blurred underwater using the Median filter based on the Biothogonal wavelet transform was presented in this paper. Research on de-noising algorithm is of considerable importance in the field of image processing, and most of the research efforts about wavelet image de-noising focus on how to select the image filter to remove the impulse noise. A Madian filter approach was proposed to remove the impulse noise in the blurred underwater image. Firstly, two-layer decomposition and reconstruction of the blurred underwater image adopting Biorthogonal basic wavelet transform was carried out. And then the Madian filter and Wiener filter were chosen to filter the blurred underwater image. Four indexes were involved to evaluation the performance of the image de-noising. Experimental results indicated that the effect of proposed Madian de-noising algorithm based on the Birthogonal wavelet in removing the noise in the underwater image is more remarkable than that of Wiener filtering.

References

[1] Santos-Victor J, Sentieiro J. *The role of vision for underwater vehicles.* Symposium on Autonomous Underwater Vehicle Technology. Cambridge. 1994: 28-35.
[2] Branca A, Stella E, Distante A. Autonomous navigation of underwater vehicles. *IEEE OCEANS.* Nice. 1998; 1:61-65.
[3] Comport I, IRISA-INRIA F, Marchand E, et al. Real-time markerless tracking for augmented reality: the virtual visual servoing framework. *IEEE Transactions on Visualization and Computer Graphics.* 2006; 12(4): 615-628.
[4] Garcia R, Nicosevici T, Cufi X. *On the way to solve lighting problems in underwater imaging.* Proceedings of IEEE Oceans Conference Record. Washington. 2002: 1018-1024
[5] Abril L, Méndez T, Dudek G. Color correction of underwater images for aquatic robot inspection. *Lecture notes in computer science.* 2005; 3757: 60–73.
[6] Gupta G. Algorithm for Image Processing Using Improved Median Filter and Comparison of Mean, Median and Improved Median Filter. *International Journal of Soft Computing and Engineering.* 2011; 1(5): 304-311.
[7] Arashloo S, Ahmadyfard A. Fine estimation of blur parmeters for image restoration. 15th International Conference on Digital Signal Processing. 2007: 427-430.
[8] Aizenberg N, Constantine B, Viktor N, et al. Blurred image restoration using the type of blur and blur parameter identification on the neural network. Image Processing: Algorithms and Systems. San Jose. 2002; 4667: 460-471.
[9] Moghaddam E. A robust noise independent method to estimate out of focus blur. *IEEE International Conference on Acoustics, Speech and Signal Processing.* Las Vegas. 2008: 1273-1276.
[10] Liu J, Qi J, Liu Z, et al. Automatic bone age assessment based on intelligent algorithms and comparison with TW3 method. *Computerized Medical Imaging and Graphics.* 2008; 32(8): 678-684.

[11] Zhang YX, Wang S, Zhang XP, el al. *Motion blurred image restoration algorithm for IC wire bonder.* International Conference on Optical Instruments and Technology: Optoelectronic Imaging and Process Technology. Shanghai. 2009; 7513: 75130C: (1-5).

[12] Zhang L, Peng ZM, Jiao J, et al. Adaptive defocus blurred image restoration based on fractional Fourier transform combining with clarity-evaluation-function. *Automatic Target Recognition and Image Analysis. Yichang.* 2009; 7495: 74954L(1-6).

[13] S Mallat. Multifrequency channel decomposition of images and wavelet models. *IEEE Transactions on Acoustics, Speech and Signal Processing.* New York. 1989; 37(12): 2091-2110.

[14] Yang R, Lin L, Gabbouj M, et al. Optimal Weighted Median Filters Under Structural Constraints. *IEEE Trans. Signal Processing.* 1995; 43: 591-604.

[15] Ng P, Ma K. A Switching Median Filter with BDND for Extremely Corrupted Images. *IEEE Trans Image Processing.* 2006; 15(6): 1506-1516.